Long-range correlations in finite nuclei: comparison of two self-consistent treatments

Y. Dewulf, D. Van Neck, L. Van Daele and M. Waroquier
Laboratory for Theoretical Physics, Proeftuinstraat 86, B-9000 Gent, Belgium

Long-range correlations, which are partially responsible for the observed fragmentation and depletion of low-lying single-particle strength, are studied in the Green's function formalism. The self-energy is expanded up to second order in the residual interaction. We compare two methods of implementing self-consistency in the solution of the Dyson equation beyond Hartree-Fock, for the case of the ^{16}O nucleus. It is found that the energy-bin method and the BAGEL method lead to globally equivalent results. In both methods the final single-particle strength functions are characterized by exponential tails at energies far from the Fermi level.

PACS: 21.10.Pc, 24.10.Cn
Keywords: self-consistent Green's function theory; single-particle spectral function

I. INTRODUCTION

The effect of nucleon-nucleon (NN) correlations on single-particle motion in finite nuclei has been the subject of many experimental and theoretical investigations [1–3]. The most striking experimental fact is the large suppression (by a factor of about 0.65 on average [2]) of the low-lying hole strength seen in $(e, e'p)$ reactions, compared to the values in the independent particle model. Both short-range (SRC) and long-range (LRC) correlations seem to play a dominant role in the observed depletion of hole strength. In order to explain this, one ususally discriminates between the effect of short-range (SRC) and long-range (LRC) correlations. Most recent calculations [4,5] now indicate that SRC, which originate from the strong short-range and tensor components of any realistic nuclear force, remove about 10% of the strength in the quasi-hole region. After accounting for the effects of SRC, which should be rather A-independent, the dynamics in the low-energy region is governed by a well-behaved effective interaction. The additional configuration mixing and coupling to collective states are known to induce a further depletion and strong fragmentation of the low-lying single-particle (s.p.) strength [6–9] . These LRC effects are dependent on the shell structure of real nuclei and cannot be extracted from nuclear matter calculations, but should be calculated explicitely for each specific nucleus.

Recently interest has arisen into *ab initio* calculations of LRC starting from realistic NN interactions [10–16]. The effects of the hard core are handled by the construction of an effective G-matrix interaction suitable for a limited model space of active nucleons in s.p. states around the Fermi level.

Especially self-consistent Green's function methods [7,8,11] have received current interest. In this context, self-consistency means that the internal lines in the self-energy diagrams should obey the Dyson equation themselves. According to fundamental theorems [17], the self-consistency requirement is necessary for the theory to obey basic conservation laws, such as conservation of energy and particle number.

The implementation of the self-consistency requirement in the description of finite nuclei, however, is not trivial. One of the problems is related to the strong non-linearity of the resulting Dyson equation, which necessitates an iterative solution. The self-energy expanded to second order in the residual interaction, *e.g.*, contains three exact propagators. If one works in a discrete model space this means that, starting from a representation of the Green's function in terms of a number N of discrete poles, the Green's function in the next iteration has a number of poles in the order of N^3, and the dimensionality quickly gets out of hand.

Two methods have been proposed to solve this problem. Van Neck *et al.* [7,8] discretized the energy axis and represented the spectral strength of the Green's function and self-energy in equidistant energy bins. This approach will be referred to as the BIN method. In the BAGEL (BAsis GEnerated by Lanczos, see [18]) approach Müther *et al.* represented [11] the Green's function in terms of a few characteristic poles, chosen in such a way that the lowest order moments of the exact distribution are reproduced.

It is not *a priori* clear that both methods give identical results when iterated to convergence. In particular, the weak point in the BAGEL method seems to be the fact that the lowest order moments of the *global* spectroscopic distribution are reproduced. It is not guaranteed that the BAGEL representation yields in all cases an accurate representation of the strength distribution in the $(A-1)$ and $(A+1)$-particle system separately. The construction of the self-energy in the next-order iteration is, however, dependent on this separation into $(A-1)$ and $(A+1)$ strength. The BIN method, on the other hand, reproduces all moments simultaneously, but only on the average due to the finite width of the employed energy bins.

It is the purpose of this letter to compare the results obtained by both methods for the case of the ^{16}O nucleus. Apart from global quantities such as the binding energy, occupation probabilities and spectroscopic factors of the main fragments, the spectral distribution in the $(A-1)$ and $(A+1)$-particle system are compared in more detail by calculating their higher order moments.

II. FORMALISM

For the purpose of a clear comparison between the two methods we make some simplifying assumptions: *(i)* We assume that the Green's function and the self-energy are both diagonal in the adopted spherical and discrete s.p. basis, *i.e.* we neglect major shell-mixing. This is justified since the energy spacing between major shells is sufficiently large to suppress mixing between s.p. states with same parity and angular momentum but different radial quantum number. The influence of major shell-mixing in the self-energy was investigated in [8] for the case of ^{208}Pb, and found to be small. *(ii)* We also ignore the residual interaction between the 2p1h and 2h1p configurations. This approximation was studied in [12,13] and will change the results only by a few percent.

The second order self-energy Σ is now represented diagrammatically in Fig. 1, and the Dyson equation to be solved takes the form

$$G_\alpha(\omega) = G^{HF}_\alpha(\omega) + G^{HF}_\alpha(\omega)\Sigma_\alpha(\omega)G_\alpha(\omega)\ , \tag{1}$$

with α the spherical s.p. label $nljm$, G the exact (second order) Green's function and G^{HF} the Hartree-Fock Green's function.

The self-consistency of our approach implies that we must use the solution $G_\alpha(\omega)$ itself in the evaluation of the self-energy $\Sigma_\alpha(\omega)$,

$$\begin{aligned}\Sigma_\alpha(\omega) = \frac{1}{2}(\frac{1}{2\pi})^2 \sum_{\gamma_1\gamma_2\gamma_3} |\langle\alpha\gamma_3|\hat{V}|\gamma_1\gamma_2\rangle_{as}|^2 \\ \times \int d\omega_1 d\omega_2 G_{\gamma_1}(\omega_1)G_{\gamma_2}(\omega_2)G_{\gamma_3}(\omega_1+\omega_2-\omega)\ .\end{aligned} \tag{2}$$

In Eq.(2) $\langle\alpha\gamma_3|\hat{V}|\gamma_1\gamma_2\rangle_{as}$ stands for the matrix elements of the effective interaction between antisymmetrized two-nucleon states. Eq.(1) with a self-energy given by eq.(2) is highly non-linear in the propagator and must be solved by iteration. Starting from a certain approximation for the Green's function, the self-energy can be evaluated using eq.(2). In the next iteration this new estimate for the self-energy is used as input in solving the Dyson equation (1) to get a new approximation for the Green's function. This iteration procedure is repeated until sufficient convergence is reached. Here, we encounter the dimensionality problem mentioned earlier: if $\Sigma^{(n)}_\alpha$ has N poles, $G^{(n+1)}_\alpha$ will have N+1 poles, and $\Sigma^{(n+1)}_\alpha$ will have a number of poles in the order of N^3, *i.e.* the number of poles is roughly cubed after each iteration. Note that this is a byproduct of the discretization of the s.p. continuum; in reality the propagator and self-energy will have, in addition to the discrete poles, branch-cuts representing the continuum states in the $(A-1)$ and $(A+1)$-particle systems. The BIN and BAGEL methods are essentially two different ways of limiting the number of poles after each iteration. For the sake of completeness we briefly summarize the two methods below. A more extensive treatment can be found in [7] and [12].

In the BIN method the energy axis is divided into a large number M_B of equidistant energy-bins (typically a few thousand). This means that in each iteration step the self-energy and Green's function are represented by their residues at a number of fixed poles, which makes it possible to develop an iterative scheme for solving eq.(1) with a self-energy given by eq.(2). The Green's function after n iterations will then be given by:

$$G^{(n)}_\alpha(\omega) = \sum_k \frac{f^{(n)}_{\alpha,k}}{(\omega - E_k + i\eta)} + \sum_k \frac{b^{(n)}_{\alpha,k}}{(\omega + E_k - i\eta)}\ , \tag{3}$$

with $E_k = k\Delta$, for $k = 1,\ldots,M_B$. Using this propagator we can calculate the self-energy $\Sigma^{(n)}_\alpha$,

$$\Sigma^{(n)}_\alpha(\omega) = \sum_k \frac{\sigma^{(+)(n)}_{\alpha,k}}{\omega - E_k + i\eta} + \sum_k \frac{\sigma^{(-)(n)}_{\alpha,k}}{\omega + E_k - i\eta}\ , \tag{4}$$

with

$$\sigma^{(+)(n)}_{\alpha,k} = \frac{1}{2} \sum_{\substack{k_1 k_2 k_3 \\ (k=k_1+k_2+k_3)}} \sum_{\gamma_1\gamma_2\gamma_3} |\langle\alpha\gamma_3|\hat{V}|\gamma_1\gamma_2\rangle_{as}|^2 f^{(n)}_{\gamma_1,k_1} f^{(n)}_{\gamma_2,k_2} b^{(n)}_{\gamma_3,k_3} \ , \tag{5}$$

$$\sigma^{(-)(n)}_{\alpha,k} = \frac{1}{2} \sum_{\substack{k_1 k_2 k_3 \\ (k=k_1+k_2+k_3)}} \sum_{\gamma_1\gamma_2\gamma_3} |\langle\alpha\gamma_3|\hat{V}|\gamma_1\gamma_2\rangle_{as}|^2 b^{(n)}_{\gamma_1,k_1} b^{(n)}_{\gamma_2,k_2} f^{(n)}_{\gamma_3,k_3} \ . \tag{6}$$

Note that the triple summation over the equidistant binpoints in eqs.(5-6) for the self-energy is in fact a triple discrete convolution, which can be performed very efficiently using Fast Fourier Transform techniques.

The next approximation for the Green's function is then given by,

$$G^{(n+1)}_{\alpha}(\omega) = \frac{1}{\omega - \epsilon^{HF}_{\alpha} - \Sigma^{(n)}_{\alpha}(\omega)} \ , \tag{7}$$

with ϵ^{HF}_{α} the Hartree-Fock s.p. energy of s.p. state α. The poles of $G^{(n+1)}_{\alpha}$ are located at the solutions ω_i of the equation

$$\omega_i = \epsilon^{HF}_{\alpha} + \Sigma^{(n)}_{\alpha}(\omega_i) \ , \tag{8}$$

and carry a strength s_i equal to

$$s_i = \frac{1}{1 - \frac{d}{d\omega}(\Sigma^{(n)}_{\alpha}(\omega))|_{\omega=\omega_i}}. \tag{9}$$

This strength is assigned to the binpoint closest to ω_i. The error coming from this averaging procedure can be made sufficiently small by choosing small widths Δ for the energy-bins.

The concept of the BAGEL approach is based on a representation of the Green's function in terms of a small number of poles, with judiciously chosen positions and residues, in such a way that the lowest order moments of the s.p. strength distribution are reproduced. Assume that the Green's function $G^{(n)}_{\alpha}(\omega)$ for each s.p. state has N poles. Then the corresponding self-energy $\Sigma^{(n)}_{\alpha}(\omega)$ will have a larger number D of poles (in the order of N^3). In the next iteration step the "true" Green's function,

$$G^{(n+1)}_{\alpha,true}(\omega) = \frac{1}{\omega - \epsilon^{HF}_{\alpha} - \Sigma^{(n)}_{\alpha}(\omega)} = \sum_{i=1}^{D+1} \frac{|X^{(n+1)}_{\alpha,i}|^2}{\omega - \omega^{(n+1)}_{\alpha,i}} \ , \tag{10}$$

will have $D+1$ poles. The moments m_p of the corresponding strength distribution are defined according to

$$m_p = \sum_{i=1}^{D+1} (\omega^{(n+1)}_{\alpha,i})^p (X^{(n+1)}_{\alpha,i})^2. \tag{11}$$

It is possible to determine a smaller set of poles, with positions and residues different from the true ones, but reproducing exactly some of the lowest-order moments m_p given in Eq.(11). The BAGEL procedure determines this smaller set by a truncated Lanczos tridiagonalisation of the Hamiltonian submatrices corresponding to the $1p \oplus 2p1h$ space and $1h \oplus 2h1p$ space. The true Green's function is then replaced by $G^{(n+1)}_{\alpha}$ containing this smaller set of poles.

Various BAGEL approximations are possible, depending on the number of Lanczos vectors constructed in the two subspaces. In the so-called BAGEL(M,M) approach, used in this work, the approximated Green's function has $(2M+1)$ poles and at each iteration step the moments m_p, for $p = 0, \ldots, 2M+1$, of the total true strength distribution will be reproduced.

III. NUMERICAL RESULTS

The construction of the effective interaction and choice of the s.p. basis are analogous to those in [12], to which we refer for more details.

We start from a realistic interaction, the Bonn-C potential [19]. The effective interaction $\hat{G}$ in ^{16}O is derived by solving the Bethe-Goldstone equation, with a Pauli operator consistent with a discrete model space of harmonic

oscillator states (with frequency $\hbar\omega_0 = 13.27MeV$) up to and including the pf shell. A value of $\omega = -30MeV$ is taken for the starting energy.

The basis of oscillator states can be identified with the Hartree-Fock basis, after subtracting from the original effective interaction a correction term [12],

$$\hat{V} = \hat{G} - \sum_{\alpha\neq\beta} (t_{\alpha\beta} + U_{\alpha\beta}) c^+_\alpha c_\beta, \tag{12}$$

in which $t_{\alpha\beta}$ stands for the matrix element of the kinetic energy operator and $U_{\alpha\beta} = \sum_h \langle \alpha h|G|\beta h\rangle_{as}$. The Hartree-Fock single-particle energies are then obtained as $\epsilon^{HF}_\alpha = t_{\alpha\alpha} + U_{\alpha\alpha}$, and are listed in Table 1.

The second order Dyson-equation is then solved self-consistently within the BAGEL and BIN methods. In both methods we use renormalized Hartree-Fock (RHF) s.p. energies in order to take the newly generated contributions to the first order self-consistent self-energy into account, *i.e.* after each iteration the s.p. energies are changed according to

$$\epsilon^{RHF}_\alpha = t_{\alpha\alpha} + \frac{1}{2} \sum_\beta n_\beta \langle \alpha\beta|\hat{V}|\alpha\beta\rangle_{as} \ , \tag{13}$$

with n_β the new occupation of the s.p. state β.

After studying the dependence of the BAGEL(M,M) approach on the number of basis vectors retained in the truncated subspaces we find that the results are converged for $M \geq 6$. We will display the results for the BAGEL(6,6) approximation. In the BIN method we used the following choice of parameters: a bin width $\Delta = 0.05MeV$ and a number of bins $M_B = 5460$.

After the first iteration the number of particles has a small (0.5%) excess. When convergence is reached the restoration of particle number conservation, typical for a self-consistent solution, is observed in both approaches. We also find that after one iteration the effect of correlations is somewhat overestimated, in agreement with the results in [7,11].

In Table 1 the RHF energies and occupation probabilites of all s.p. states are shown. These are in complete agreement for the two methods. The same agreement holds for the mean removal energies (not shown in Table 1), and hence also for the total binding energy per nucleon, calculated via the Koltun sum rule, which is listed on the last row in Table 1.

In the last columns of Table 1 we compare the position and strength of the main fragment in both methods. The valence shells ($1p$, $2s$, $1d$) have a clear quasi-particle/hole behaviour, with one pole carrying about 90% of the total s.p. strength. The positions and strengths of these states are equivalent in both approaches. A more detailed comparison reveals that the strengths of the largest peaks are systematically higher in the BAGEL approach than in the BIN method, an effect that becomes more pronounced away from the Fermi level. This is due to the fact that in the BAGEL approach, because of the limited number of poles, the main peaks need to carry some additional strength corresponding to states which in the BIN method are really separate states, *i.e.* the BIN method allows for more fragmentation.

This is seen more clearly in Fig. 2, where the total spectral functions of the $1s_{1/2}$ and $1d_{5/2}$ states are shown. Apart from this enhanced fragmentation into discrete states for energies up to about 30 MeV above and below the Fermi level, one also observes for larger energies the appearance of a quasi-continuous distribution in the BIN results. This part of the distribution is of course also represented in the BAGEL method, in terms of a few well-separated states.

A very surprising feature, appearing in both the BAGEL and BIN methods, is the nearly perfect exponential decay of the spectral function at these large excitation energies. The decay constant has the same value in both methods. To within a few percent, this value is independent of the s.p. state, and the same for the strength tails in the $(A+1)$ and $(A-1)$ system. Since the determination of the Green's function in each iteration step only involves rational functions, the exponential behaviour must be built up by the iterative procedure itself, *i.e.* it is a genuine result of the requirement of self-consistency for the Green's function. We do not know whether it is also a general feature of the exact Green's function, without two limitations of the present model: *(i)* The G-matrix is used here as a static effective interaction [12]. In principle the energy-dependence of the G-matrix must be taken into account for large excitation energies in the $(A \pm 1)$ system, and this may affect the behaviour of the spectral function in this energy domain. *(ii)* The s.p. continuum is discretized, and is represented in terms of a few unoccupied s.p. states, *i.e.* we work in a truncated model space. It is unclear whether the exponential decay of the iterated spectral function would persist if already in the first iteration step, on the 2p1h-2h1p level, the self-energy strength is spread out over all energies (as will be the case with an exact treatment of the continuum).

The exponential localization of strength distributions in a finite model space was also found in a recent investigation [20], where the statistical properties of the $J^\pi T = 0^+0$ states for 16 active nucleons in the sd shell were studied. This

feature seems to be poorly understood at present. Note that self-consistent Green's function methods, which include many-body damping in a natural way [7], can also provide a dynamical framework for the process of stochastization in complex wavefunctions. It should *e.g.* be possible to derive the localization length directly in our model. Work along these lines is in progress.

In Fig. 3 the detailed behaviour of the $(A-1)$ part of the $l=1$ spectral function is shown in the energy region above the quasi-hole peaks. The spectral functions have been folded with a Lorentzian having a full width of 1 MeV. In the BAGEL approach the spectral strength is characterized by two peaks of about the same energy, whereas in the BIN approximation a broader distribution appears with a natural spreading width.

The BAGEL(M,M) method reproduces, at each iteration step, the moments of the total strength distribution up to order $2M+1$. This property, however, is not conserved through succesive iterations, since the self-energy depends on the separation of the spectral function into its $(A-1)$ and $(A+1)$ parts. So strictly speaking there is no exact relationship between the moments of the true (converged) spectral function and its BAGEL approximation, though in practice the BAGEL property is so restrictive that also the separate $(A-1)$ and $(A+1)$ parts will be, in most cases, well described in terms of a few BAGEL states. This holds especially for fairly weakly correlated Fermi systems, where the spectral function is dominated by either the $(A-1)$ or $(A+1)$ part, since in that case the reproduction of the moments of the total spectral function and of those of its dominant part is practically coinciding.

In order to study this point it is interesting to compare the moments of the BAGEL spectral functions with those obtained with the BIN method, since in the latter approach the errors due to averaging are expected to be spread evenly over the entire energy range. In Table 2 we list the relative differences between the central moments of the $(A-1)$, $(A+1)$ and total s.p. strength distribution, obtained in both methods. The agreement for the total distribution is impressive, with deviations of less than 1% up to the sixth moment. The same holds for the moments of the dominant part of the distribution (the $(A-1)$ part for the hole states, the $(A+1)$ part for the particle states), whereas the deviations for the non-dominant part are somewhat larger. Only for the highest moments the two methods start to deviate substantially.

For future applications that go beyond the second-order level it is also of interest to compare the numerical workload required by both methods. Of course this workload depends crucially on the number of Lanczos vectors in BAGEL or on the number of energy bins in the BIN method. For the present choice of parameters the computational effort is of similar magnitude for both methods, if Fast Fourier Transform is used in the BIN method to evaluate the discrete convolutions in eqs.(5-6) (this was not implemented in earlier calculations [7,8]). The storage requirement for the Green's function, however, is considerably less in the BAGEL method (in which the Green's function is represented by a small number of poles and residues) than in the BIN method (in which the value of the spectral function at each energy binpoint must be stored).

IV. SUMMARY

We compared two theoretical methods, that aim at implementing the important requirement of self-consistency in the framework of Green's function theory, by calculating the single-particle spectral functions in ^{16}O. We found that they yield equivalent results for all global quantities that depend on the lowest order moments, such as occupation probabilities, mean removal energies and total binding energy. The prediction for the strength and position of the valence state quasi-particle/hole peak are also in close agreement. The BIN method allows for more fragmentation resulting in structures at intermediate energies that have a natural spreading width.

In both methods the spectral functions exhibit an exponential decay at large excitation energies in the $(A-1)$ and $(A+1)$ system. It is likely that this is a result of the requirement of self-consistency.

Acknowledgments

This work is supported by the Fund for Scientific Research - Flanders (FWO). We are grateful to H. Müther for providing us with the G-matrix elements used in this work.

[1] P.K.A. de Witt Huberts, Nucl. Phys. **A507** (1990) 189c

[2] L. Lapikas, Nucl. Phys. **A553** (1993) 297c
[3] C. Mahaux and R. Sartor, Adv. Nucl. Phys. **20** (1991) 1
[4] M. Radici, S. Boffi, S.C. Pieper and V.R. Pandharipande, Phys. Rev. **C50** (1994) 3010
[5] H. Müther and W.H. Dickhoff, Phys. Rev. **C49** (1994) R17
[6] D. Van Neck, J. Ryckebusch and M. Waroquier, Phys. Lett. **B249** (1990) 157
[7] D. Van Neck, M. Waroquier and J. Ryckebusch, Nucl. Phys. **A530** (1991) 347
[8] D. Van Neck, M. Waroquier, V. Van der Sluys and K. Heyde, Nucl. Phys. **A563** (1993) 1
[9] V. Van der Sluys, D. Van Neck, M. Waroquier and J. Ryckebusch, Nucl. Phys. **A551** (1993) 210
[10] H. Müther and L.D. Skouras, Nucl. Phys. **A555** (1993) 541
[11] H. Müther and L.D. Skouras, Phys. Lett. **B306** (1993) 201
[12] H. Müther and L.D. Skouras, Nucl. Phys. **A581** (1995) 247
[13] K.M. Amir-Azimi-Nili, H. Müther, L.D. Skouras and A. Polls, Nucl. Phys. **A604** (1996) 245
[14] M.G.E. Brand, G.A. Rijsdijk, F.A. Muller, K. Allaart and W.H. Dickhoff, Nucl. Phys. **A531** (1991) 253
[15] G.A. Rijsdijk, K, Allaart and W.H. Dickhoff, Nucl. Phys. **A550** (1992) 159
[16] W.J.W. Geurts, K. Allaart, W.H. Dickhoff and H. Müther, Phys. Rev. **C53** (1996) 2207
[17] G. Baym and L.P. Kadanoff, Phys. Rev. **124** (1961) 287; L.P. Kadanoff and G. Baym, *Quantum Statistical Mechanics*, Benjamin, New York 1962
[18] H. Müther, T. Taigel and T.T.S. Kuo, Nucl. Phys. **A482** (1988) 601
[19] R. Machleidt, Adv. Nucl. Phys. **19** (1989) 189
[20] N. Frazier, B.A. Brown and V. Zelevinsky, Phys. Rev. **C54** (1996) 1665

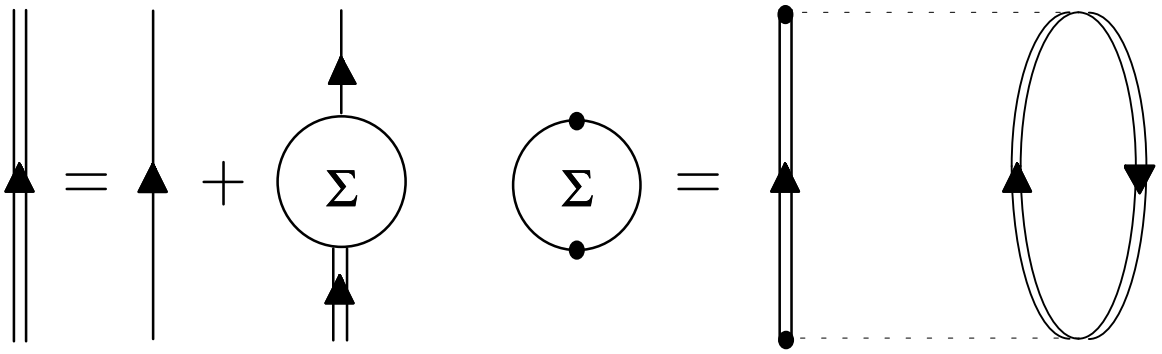

Fig. 1

FIG. 1. Diagrammatical representation of second order self-consistent Dyson equation

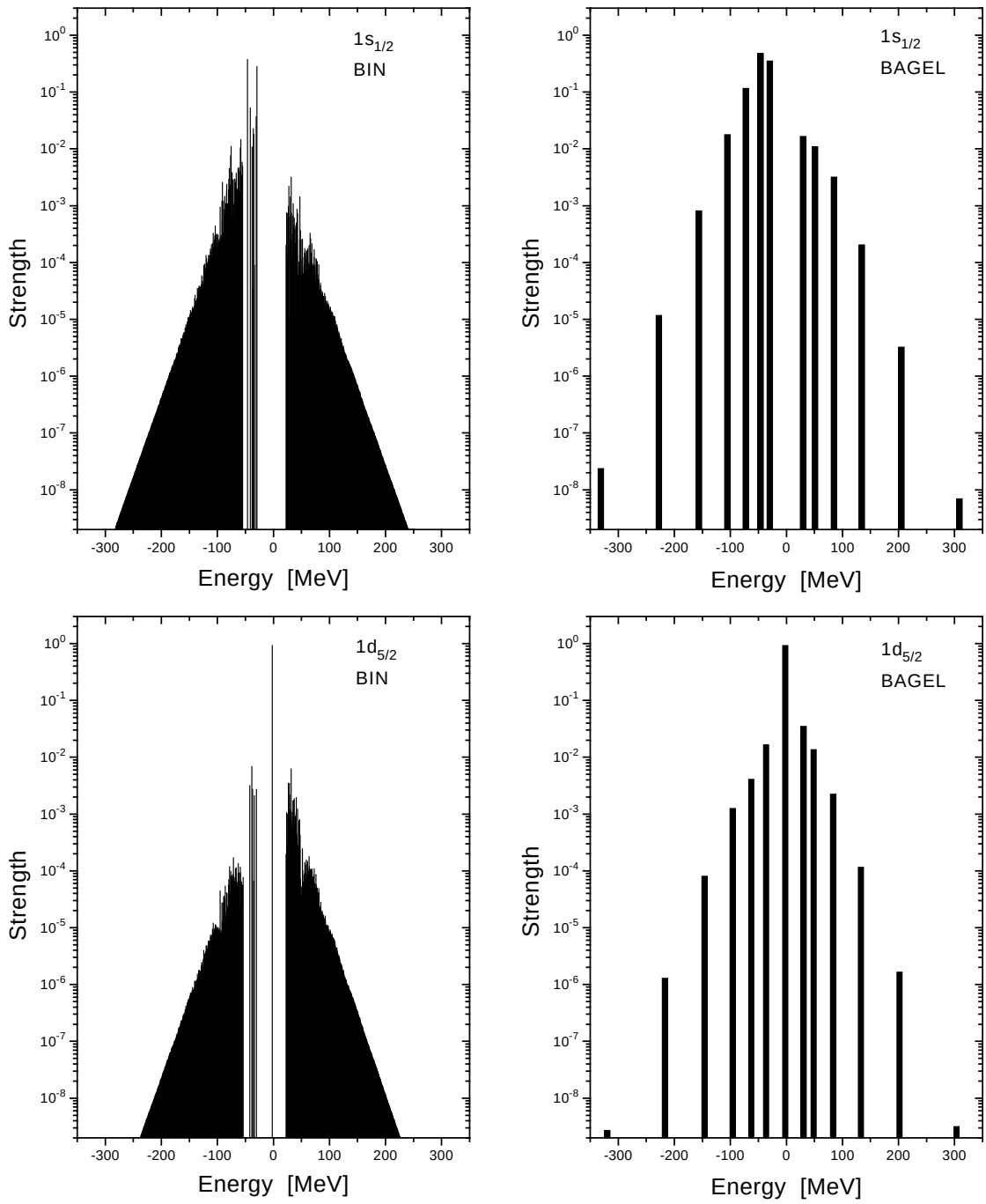

Fig.2

FIG. 2. Total (discrete) spectral function for the $1s_{1/2}$ and $1d_{5/2}$ s.p. states in ^{16}O, obtained with BIN and BAGEL method, after convergence. For practical reasons the strength has been resummed in intervals of 0.25 MeV for the BIN result.

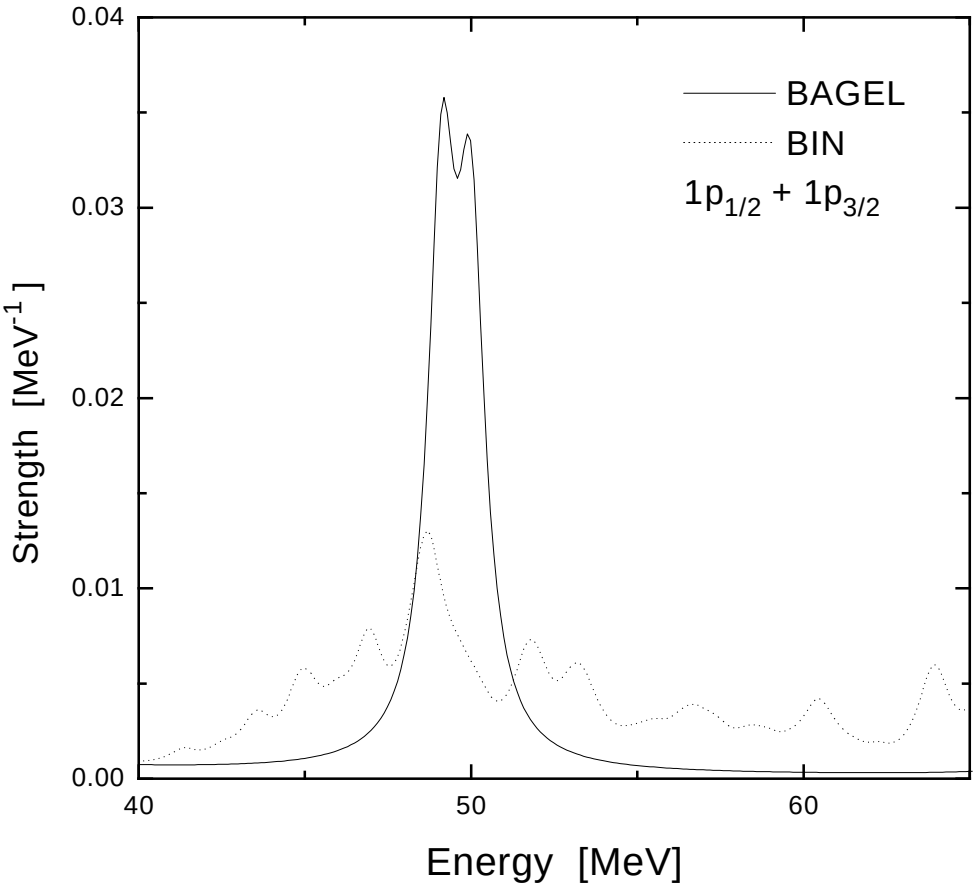

Fig.3

FIG. 3. Spectral function for $l = 1$ strength in the $A = 15$ system. The discrete spectral function has been folded with a Lorentzian having a full width of 1 MeV.

TABLE I. The HF energy ϵ_α^{HF}, RHF energy ϵ_α^{RHF}, occupation probability n_α, the spectroscopic factor and position of the largest fragment for all s.p. states in ^{16}O, in the BAGEL and the BIN approximation. All energies are in MeV. All other entries are fractions of the degeneracy $(2j+1)$

		BAGEL	BIN	BAGEL	BIN	BAGEL		BIN	
state	ϵ_α^{HF}	ϵ_α^{RHF}	ϵ_α^{RHF}	$n_\alpha(\%)$	$n_\alpha(\%)$	E_{max}	$R_{max}(\%)$	E_{max}	$R_{max}(\%)$
$1s_{1/2}$	-42.93	-41.64	-41.63	96.89	96.89	-45.96	47.80	-46.18	37.60
$1p_{3/2}$	-20.14	-19.38	-19.38	94.99	94.98	-19.56	88.43	-19.53	88.38
$1p_{1/2}$	-16.47	-15.85	-15.85	93.81	93.79	-16.18	87.59	-16.18	87.54
$1d_{5/2}$	-1.295	-0.9692	-0.9678	2.22	2.22	-2.075	92.63	-2.084	92.61
$2s_{1/2}$	-0.6594	-0.3901	-0.3895	1.89	1.90	-1.888	91.57	-1.884	91.54
$1d_{3/2}$	4.119	4.284	4.284	2.66	2.66	2.775	89.05	2.766	88.98
$1f_{7/2}$	13.65	13.74	13.74	0.27	0.27	9.616	63.96	9.366	56.57
$2p_{3/2}$	10.96	11.22	11.22	0.89	0.89	9.108	78.53	8.966	72.28
$1f_{5/2}$	19.08	19.05	19.05	0.59	0.59	22.36	50.34	13.87	20.82
$2p_{1/2}$	12.66	12.91	12.91	0.83	0.83	10.36	74.77	10.12	64.79
E/A						-6.413 MeV		-6.408 MeV	

TABLE II. Relative differences between the central moments of s.p. strength distributions obtained in the BAGEL and the BIN approximation, separately for the distributions in the $(A-1)$ system ($\Delta\mu^{<}$), in the $(A+1)$ system ($\Delta\mu^{>}$), and for the total distribution ($\Delta\mu$).

	$1s_{1/2}$			$1d_{5/2}$		
k	$\Delta\mu_k^{<}(\%)$	$\Delta\mu_k^{>}(\%)$	$\Delta\mu_k(\%)$	$\Delta\mu_k^{<}(\%)$	$\Delta\mu_k^{>}(\%)$	$\Delta\mu_k(\%)$
2	$3.096\ 10^{-3}$	-0.1080	$1.093\ 10^{-3}$	-0.6887	$-4.946\ 10^{-2}$	$-1.094\ 10^{-2}$
4	$8.008\ 10^{-2}$	0.1066	$4.062\ 10^{-2}$	-0.2463	$4.810\ 10^{-2}$	0.1024
6	0.6429	2.151	0.1741	2.362	0.4823	0.5601
8	3.319	9.303	0.7806	10.27	2.600	2.646
10	11.29	26.18	2.909	28.43	9.228	9.046